JOURNAL OF CATALYSIS 41, 440–454 (1976)

Kinetics of NH_3 Decomposition on Polycrystalline Pt[1]

D. G. LÖFFLER AND L. D. SCHMIDT

Department of Chemical Engineering and Materials Science, University of Minnesota, Minneapolis, Minnesota 55455

Received June 4, 1975

The kinetics of NH_3 decomposition on polycrystalline Pt are examined over a wide range of catalyst temperature ($500 < T < 1700$°K), pressure ($0.015 < P_{NH_3} < 20$ Torr), and gas composition in a steady-state flow system with conversions sufficiently low that differential rates are obtained. Calibration of system and mass spectrometer parameters yields an apparent accuracy of better than ±10% under all conditions. All data in pure NH_3 and in NH_3–H_2 and NH_3–N_2 mixtures could be fit to a single Langmuir–Hinshelwood (LH) rate expression with experimental data deviating from calculated LH curves by less than 10% in pure NH_3 and 20% in NH_3–H_2 mixtures over a range of 10^4 in reaction rates. Orders with respect to NH_3, H_2, and N_2 are determined, and coefficients of pressures are shown to have Arrhenius temperature dependences with activation energies appropriate for heats of adsorption. Several reaction mechanisms which can give this rate expression are described, and the significance of parameters is discussed.

INTRODUCTION

Because of its apparent simplicity and assumed relation to NH_3 synthesis, the catalytic decomposition of NH_3 on transition metals, especially Fe and Pt, has been examined many times over the last 50 years (*1, 2*). Kinetic measurements on Pt in batch (*3–6*) and flow (*7, 8*) reactors yield qualitatively similar results with respect to orders of reaction for NH_3, H_2, and N_2 and the activation energy, but deviations from the mean are frequently large (*2*). Rates are typically fit to Temkin–Pyzhev expressions (*2, 9*), although agreement of any set of data with this expression is obtained only by letting some of the constants be functions of temperature and partial pressures, and many alternate rate expressions have been proposed (*1, 2*). Various investigators have attempted to show the adsorbed complex to be N atoms, NH, NH_2, or NH_3 by analysis of kinetics. (It should be noted that in most previous studies the principal interest was the synthesis reaction on Fe, and the kinetics of the decomposition on Pt has not received comparable attention.) Recent interest has centered on direct examination of these complexes by mass spectrometric analysis of desorption products (*10*) or of fragments desorbed by ion impact (*11*). While in principle more direct than kinetic analysis, these experiments have also been frustrated by uncertainties in interpretation of the results.

In the work reported here we find that rates of NH_3 decomposition over a wide range of temperature and partial pressures of NH_3, H_2, and N_2 can be fit to a single Langmuir–Hinshelwood (LH) rate expression. This expression also fits the data of most previous investigations, but it elimi-

[1] This work was partially supported by NSF under grants No. GK16241 and ENG75-01918.

nates the need for many of the complex assumptions invoked to explain data obtained over limited ranges of temperature, gas composition, and conversion.

These results agree with our previous contention that LH kinetics qualitatively predict measured rates of CO oxidation (*12*), NH_3 decomposition (*13*), the NO + NH_3 reaction (*13*), and NH_3 oxidation on Pt, Pd, and Rh (*14*). The emphasis in the present work is to obtain rates in this simple reaction as accurately as possible in order to measure all rate parameters, to test quantitatively the validity of LH kinetics, and to obtain adsorption, desorption, and reaction parameters.

EXPERIMENTAL

Reaction rates in a Pyrex steady-state flow reactor were measured continuously with a differentially pumped quadrupole mass spectrometer system. While the apparatus and procedures have been described previously in connection with steady-state and transient kinetics of NH_3 and CO oxidation reactions (*12*, *13*), the accuracy and precision of measurements have been improved by more careful specification of partial pressures, temperatures, and reactor parameters.

Gases were admitted through metal valves, and all inlet and outlet flow lines were trapped with liquid nitrogen or Dry Ice. The catalyst was an 8-cm length of 0.025-cm-diameter high purity polycrystalline Pt wire. Short segments of 0.0075-cm-diameter wire were welded between the wire and its supports for uniform temperatures, and temperatures were measured from the resistance between 0.0075-cm-diameter potential leads. A Kelvin bridge temperature controller maintained specified temperatures constant to within a few degrees.

After heating in O_2 at $\sim$1 Torr for several minutes to remove carbon, rates of NH_3 decomposition were reproducible to within a few percent on a given wire and within 10% over long periods of time and on several different wires. Wires were periodically heated in O_2, but there was never any evidence of contamination after many hours of reaction as long as high purity gases were used with trapping. Wires were frequently heated to high temperatures, and their shiny appearance and previous examination with scanning electron microscopy (*15*) indicated them to be smooth. The reproducibility of data and examination by Auger electron spectroscopy and sputtering techniques are evidence that Pt surfaces heated in O_2 are "clean," i.e., are free of carbon, sulfur and other typical contaminants (*16*). We interpret the present results in NH_3 and H_2 mixtures as also indicative of contaminant-free surfaces. This implies that the high H_2 pressures in reducing atmospheres are also efficient in removing traces of C and S which must be present in the gases in the parts-per-million range. We emphasize that we have no direct evidence that these surfaces are clean, and further experiments are necessary to determine species coverages directly.

Rates were measured using the "stirred tank" mass balance equation,

$$r_R = (q/(ART_g))(P_{j0} - P_j), \qquad (1)$$

where r_R is the reaction rate per unit surface area A, q is the volumetric flow rate, and P_{j0} and P_j are the inlet and reactor partial pressures of species j. The flow rates of reactants were obtained by measuring the rate of pressure decrease in flasks with gases leaking into the reactor. Absolute total pressures were measured with a trapped McLeod gauge connected to the reactor. Measurement of pressure versus flow rates in gas mixtures confirmed that the composition in the reactor was that fixed by the flow rates, i.e., that the residence times for all gases were identical. Mass spectrometer sensitivities were determined for each gas at the composition of

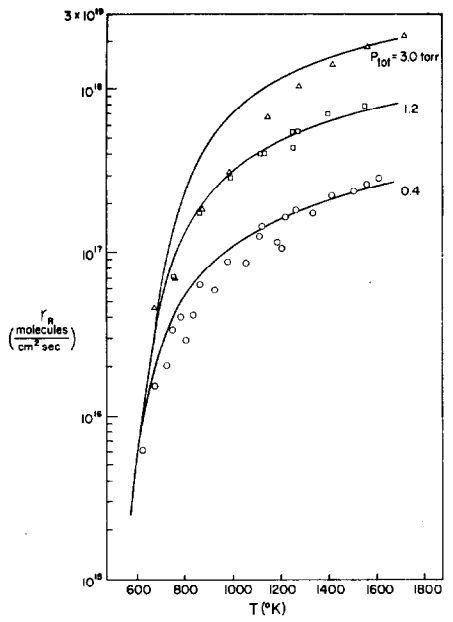

FIG. 1. Rate of decomposition r_R on Pt versus T in a mixture of 25% NH_3 and 75% Ar at total pressures indicated. Rates are within a few percent of those in pure NH_3 at the same partial pressure (solid curves) at high temperature, indicating no boundary layer depletion up to those pressures.

interest by switching from a given reactant composition to one containing a small known percentage of the product being monitored (N_2 with pure NH_3 or NH_3/H_2 mixtures and H_2 with NH_3/N_2 mixtures). This corrects for variations in mass spectrometer sensitivity which can be as much as 50% in widely different gas compositions.

Conversions were always less than 5% for $T < 800$°C and less than 15% at the highest temperatures so that rates in Eq. (1) are nearly those of a *differential* reactor. This was especially important at low temperatures where product H_2 severely inhibits the reaction. Measurement at low conversions required accurate suppression of background partial pressures in the mass spectrometer. Product inhibition affected the rates of NH_3 decomposition reported previously (*13*, *14*) and may have been significant in NH_3 oxidation also because conversions as high as 50% were used.

The residence time, controlled by a valve between the reactor and the pump, was typically less than 1 sec. Steady-state rates were attained within the 1–3-sec response time of the recorder following any step changes in temperature and composition.

Use of Eq. (1) requires that the gas composition be uniform. For pressures <1 Torr the mixing time in a 10-cm-diameter bulb is <0.06 sec, much less than the residence time. However for high reaction rates and high pressures there may be reactant depletion near the wire surface because of boundary layer diffusion limitations at pressures where viscous flow applies. Calculations are difficult because of possible convection, but we suggested previously that boundary layer depletion may have been significant in NH_3 oxidation above 0.1 Torr for high reaction rates (*13*, *14*).

The onset of boundary layer depletion of reactant was examined by measuring the apparent rate of NH_3 decomposition by dilution with Ar. Figure 1 shows that for a composition of 25% NH_3 and 75% Ar, the reaction rates at high temperatures do not fall below the rate in pure NH_3 (solid lines) at the same partial pressure up to a pressure of 3.0 Torr. At lower temperatures the rate appears to be somewhat lower than in pure NH_3, but these differences are within the accuracy of these early data. This result demonstrates that the stirred tank flow reactor method is applicable up to at least 1 Torr for reaction probabilities above 0.01 (see below). It also indicates that the method has sufficient accuracy to permit determination of possible inhibition by N_2 and H_2 added in large excess of the NH_3.

DECOMPOSITION OF PURE NH_3

Figure 2 shows the rate of NH_3 decomposition versus Pt wire temperature

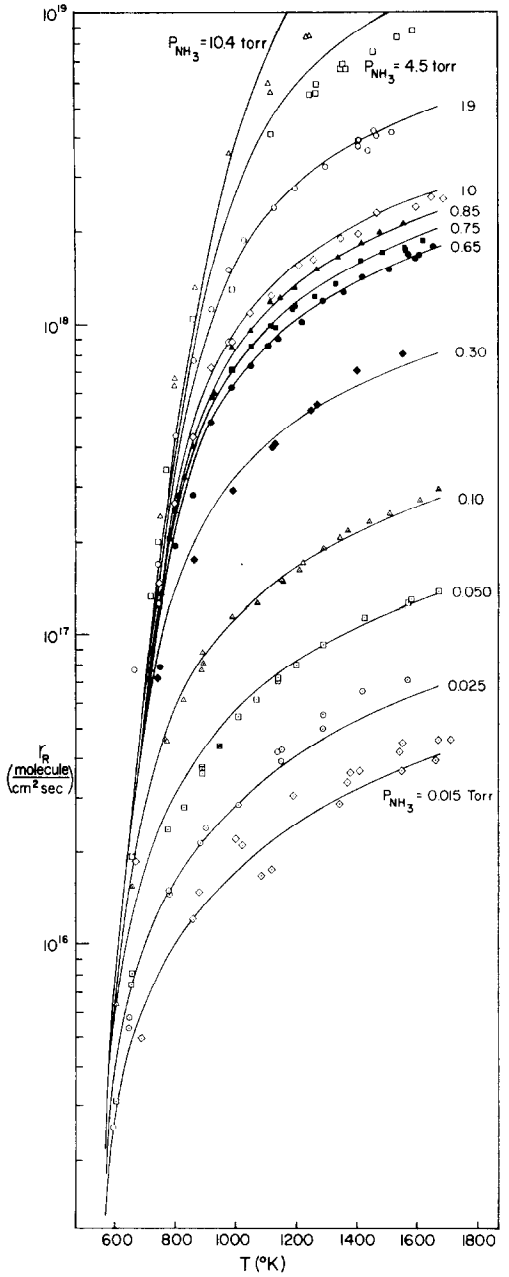

FIG. 2. Rates of NH_3 decomposition on Pt in pure NH_3 between 0.015 and 10 Torr versus temperature. Conversions were sufficiently low that differential rates are obtained. The solid curves are *calculated* from the Langmuir–Hinshelwood unimolecular reaction rate expression, Eq. (2).

for NH_3 pressures between 0.015 and 10.4 Torr. At low temperatures the rates at all pressures obviously follow an asymptote,

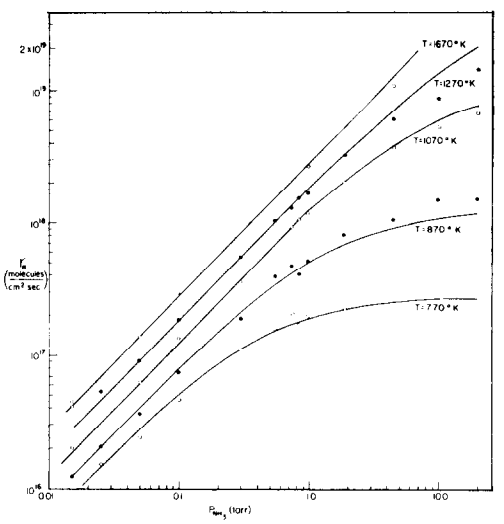

FIG. 3. Plot of log r_R versus log P_{NH_3} for temperatures indicated. At high temperatures the reaction is first order in P_{NH_3} and at low temperatures the reaction rate becomes independent of P_{NH_3} as predicted by Eq. (2) (solid curves).

showing that the reaction is zeroth order with respect to P_{NH_3}. At high temperatures the rates drop below the asymptote and become dependent on pressure. Figure 3 shows a plot of rate versus P_{NH_3} for temperatures shown. Data points in the isotherms are points from Fig. 2 if they coincide with the temperature chosen; otherwise rates were interpolated from rates just above and below that temperature. The rate is first order in P_{NH_3} at high temperatures ($m_{NH_3} = 0.99 \pm 0.05$) and approaches zeroth order at high pressure for the low temperature isotherms. This indicates that the rate in pure NH_3 should be given by a LH rate expression,

$$r_R = k_R K_{NH_3} P_{NH_3} / (1 + K_{NH_3} P_{NH_3}), \quad (2)$$

where k_R is usually interpreted as the reaction rate constant

$$k_R = k_{0R} \exp(-E_R/RT) \quad (3)$$

and K_{NH_3} the adsorption constant for NH_3,

$$K_{NH_3} = K_{0NH_3} \exp(E_{NH_3}/RT), \quad (4)$$

with E_R and E_{NH_3} the activation energy for reaction and the heat of adsorption of NH_3, respectively.

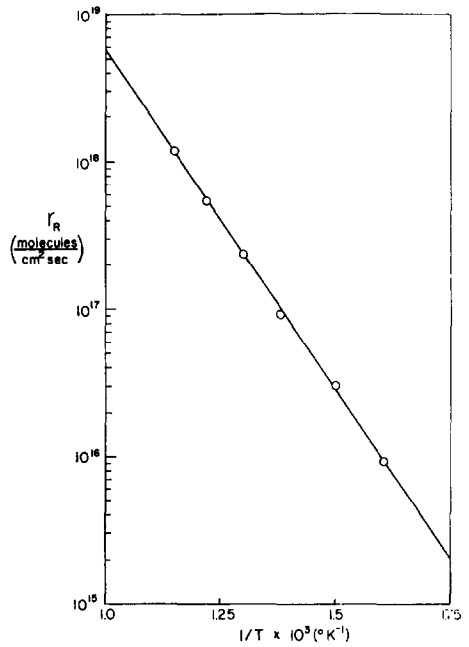

FIG. 4. Plot of log r_R versus $1/T$ in pure NH_3 for the data of Fig. 2 in the zero-order regime. The slope and intercept of this line gives k_R as shown in Eq. (5).

The Arrhenius forms of k_R and K_{NH_3} are examined in Figs. 4 and 5. Figure 4, obtained from points on the zero-order asymptote of Fig. 2, gives a straight line for a rate variation by a factor of 100. This yields

$$k_R\left(\frac{\text{molecules}}{\text{cm}^2\ \text{sec Torr}}\right) = 2.27 \times 10^{23} \exp(-21{,}000/RT), \quad (5)$$

with E_R in calories per mole. A plot of r_R/P_{NH_3} versus $1/T$ for the high temperature rates is shown in Fig. 5. While the variation in r_R/P_{NH_3} is only over a factor of two (temperature range limited by vaporization of Pt), data appear to follow the Arrhenius form with

$$k_R K_{NH_3}\left(\frac{\text{molecules}}{\text{cm}^2\ \text{sec Torr}}\right) = 9.87 \times 10^{18} \exp(-4300/RT), \quad (6)$$

or, using Eq. (5),

$$K_{NH_3}(\text{Torr}^{-1}) = 4.35 \times 10^{-5} \times \exp(16{,}700/RT). \quad (7)$$

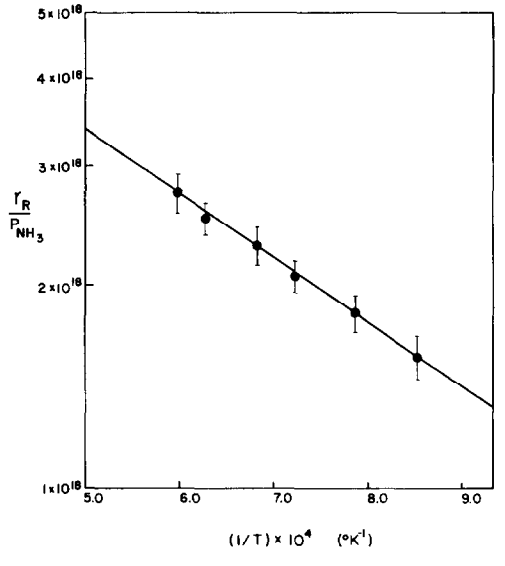

FIG. 5. Plot of log r_R/P_{NH_3} versus $1/T$ in pure NH_3 in the high temperature first-order regime. The slope and intercept of this line give $k_R K_{NH_3}$ as shown in Eq. (6).

Solid lines in Figs. 2 and 3 are those *calculated* from Eq. (2) with parameters from Eq. (5) and (7). *Rates over a factor of 10^4 are fit by this expression with no systematic deviations.* Excepting the high pressure curves, P_{NH_3} = 10.4 and 4.5 Torr, and the lowest pressure, 0.015 Torr, the largest deviation of any point from the calculated curves is ~10%. At 0.015 Torr the curves exhibit random scatter because of pressure measurement inaccuracies. At high pressures the actual rates are consistently below the calculated rates, but this is certainly due to either the reverse reaction or pressure decrease near the wire surface (Fig. 1). Equilibrium with H_2 and N_2 would at first sight appear to be far toward NH_3 at these relatively high temperatures. However in the approximation of a well-mixed reactor (low pressure), the temperature relevant to an equilibrium composition calculation is *room temperature* because that is the temperature of most of the gas in the reactor. This rather sur-

prising result can be seen simply by writing the reversible adsorption, reaction, and desorption steps

$$NH_3(g, 300°K) \rightleftarrows NH_3(s, T)$$
$$NH_3(s, T) \rightleftarrows N(s, T) + 3H(s, T)$$
$$N(s, T) \rightleftarrows \tfrac{1}{2}N_2(g, 300°K)$$

and

$$3H(s, T) \rightleftarrows \tfrac{3}{2}H_2(g, 300°K).$$

If all of these steps are at equilibrium, then their sum,

$$NH_3(g, 300°K) \rightleftarrows \tfrac{1}{2}N_2(g, 300°K) + \tfrac{3}{2}H_2(g, 300°K),$$

will be at equilibrium. This indicates that this reactor type may be useful in the study of other exothermic reaction rates at high temperatures because the equilibrium limitation is that at room temperature as long as the pressure is sufficiently low. If there are significant temperature and composition variations in the boundary layer, the relevant limitation is of course at that temperature and composition.

Equilibrium for $P_{NH_3} = 10.4$ Torr yields $P_{N_2} = 1.1$ Torr, which is significant compared to $P_{N_2} = 0.4$ Torr which corresponds to the measured conversion of 8%. Thus, we conclude that in pure NH_3 there are no detectable systematic deviations in the actual reaction rate from the above expression.

HYDROGEN INHIBITION

Next, rates were measured with mixtures of NH_3 and H_2 to determine the influence of H_2 on the decomposition rate. Figure 6 shows r_R versus T for NH_3 pressures of 0.05, 0.3, and 0.65 Torr with hydrogen pressures as indicated. Similar sets of data were obtained for additional NH_3 pressures, but for clarity they are not shown in Fig. 6.

We assumed that in H_2 or N_2, the rate expression in pure NH_3 should be modified

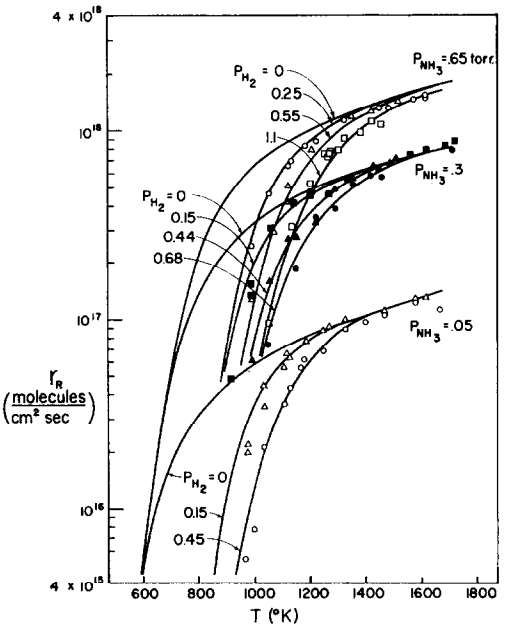

FIG. 6. Plot of r_R versus T in NH_3–H_2 mixtures for three pressures of NH_3 and for H_2 pressures indicated. Solid curves are those calculated from an expression of the form of Eq. (8) with parameters shown in Eq. (12).

by adding terms in the denominator of Eq. (2) to obtain

$$r_R = k_R K_{NH_3} P_{NH_3} / (1 + K_{NH_3} P_{NH_3} + K_H P_{H_2}{}^{m_H} + K_N P_{N_2}{}^{m_N}). \quad (8)$$

Mechanisms which yield these rate expressions with various values of m_H and m_N will be discussed later.

With $P_{N_2} = 0$ solution of Eq. (8) for $K_H P_{H_2}{}^{m_H}$ yields

$$K_H P_{H_2}{}^{m_H} = k_R K_{NH_3} P_{NH_3} \left(\frac{1}{r} - \frac{1}{r_0}\right), \quad (9)$$

where r_0 is the rate of reaction with $P_{H_2} = 0$, Eq. (2). Rates in Fig. 6 were plotted as a function of P_{H_2} as shown in Fig. 7 for three different temperatures. As with isotherms in pure NH_3, data points at the indicated temperatures were extrapolated from data at temperatures just above and below those of interest. These points give

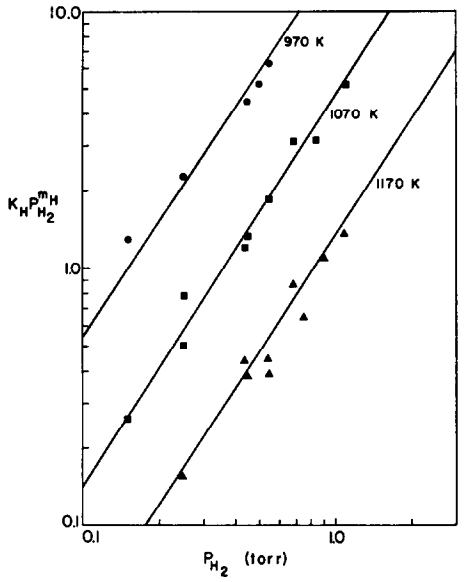

FIG. 7. Plot of log $K_H P_{H_2}^{m_H}$ as defined by Eq. (8) and (9) versus log P_{H_2} at temperatures indicated. The solid lines are those predicted for $m_H = \frac{3}{2}$, and the best fit to these data gives $m_H = 1.5 \pm 0.3$.

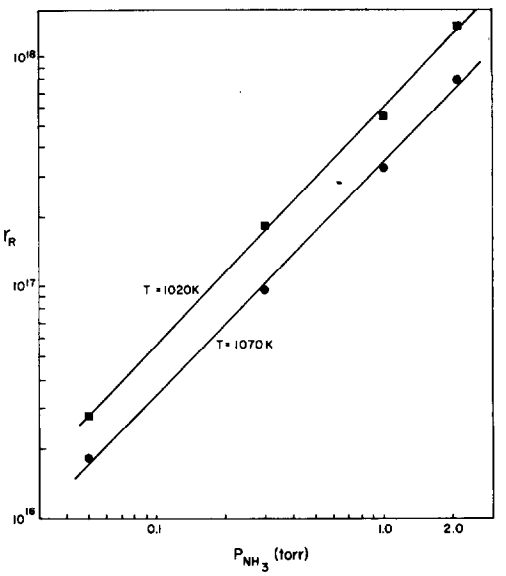

FIG. 8. Rate of reaction versus P_{NH_3} in a hydrogen pressure of 0.45 Torr. The lines drawn through the data points indicate a first-order dependence on P_{NH_3}.

straight lines on the log–log plot and the slopes of these lines give $m_H = 1.5 \pm 0.30$.

The dependence of r_R on P_{NH_3} for a fixed P_{H_2} of 0.45 Torr and two temperatures is shown in Fig. 8. It is evident that the rate is precisely first order in P_{NH_3} over a pressure variation by a factor of ~ 100.

The temperature dependence of K_H was determined by dividing the quantity $K_H P_{H_2}^{m_H}$ of Eq. (9) by $P_{H_2}^{\frac{1}{2}}$, and Fig. 9 shows a plot log K_H versus $1/T$. This indicates that K_{H_2} can be fit by an Arrhenius temperature dependence with

$$K_H \left(\frac{\text{molecules}}{\text{cm}^2\,\text{Torr}}\right) = 9.85 \times 10^{-6} \exp\,(27{,}700/RT). \quad (10)$$

All solid lines in Fig. 6 are those *calculated* assuming the form of Eq. (8) with Arrhenius parameters from Eqs. (6), (7), and (10). The experimental scatter of data points is larger than for pure NH_3, as expected, because rates in H_2 are lower, they depend more strongly on temperature, and an additional experimental parameter must

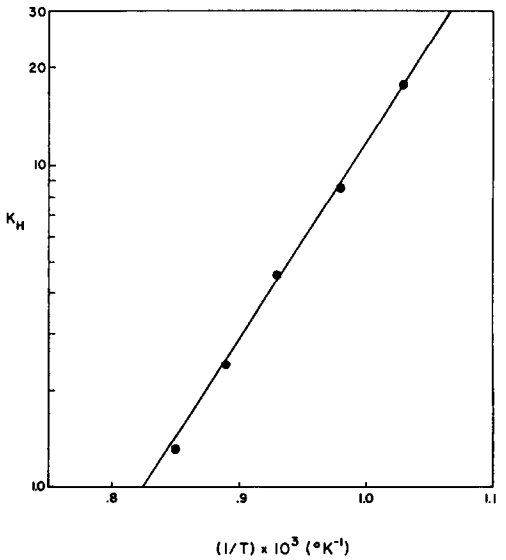

FIG. 9. Plot of log K_H, defined by Eq. (9), versus $1/T$. A straight line indicates that the hydrogen adsorption constant K_H has an Arrhenius form, and parameters are shown in Eq. (10).

be specified. However no data points shown in Fig. 6 or any other data not shown deviated from the calculated curves by more than ~20%, and no systematic deviations of any points from the calculated curves are evident.

We attempted to observe D_2 inhibition of NH_3 decomposition. However the rate was approximately the same as with H_2 at identical pressures, and our accuracy was not sufficient to resolve the expected differences of ≤ 2 between the isotopes. We also attempted to search for lack of equilibration of D and H in the hydrogen decomposition products. These measurements were frustrated by the rapid equilibrium in the $H_2 + D_2$ reaction on Pt. With a system pumping time constant of ~0.1 sec, HD was detected even at room temperature (reaction was stopped by cooling the Pt to 78°K), and a near-equilibrium distribution of hydrogen isotopes was obtained for $T > 500$°K.

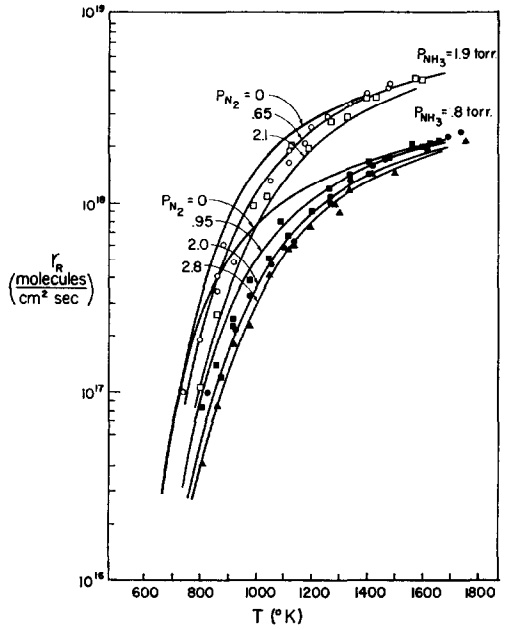

FIG. 10. Plot of log r_R versus T in NH_3–N_2 mixtures for values of P_{NH_3} and P_{N_2} as indicated. Solid curves are calculated from Eq. (12), and the upper curves in each set are for pure NH_3 at the same partial pressures.

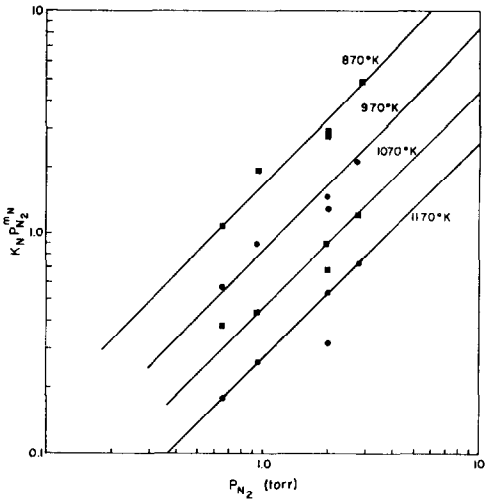

FIG. 11. Plot of log $K_N P_{N_2}^{m_N}$, defined by Eq. (11), versus log P_{N_2}. The slopes of these lines give $m_N = 1.0$.

NITROGEN INHIBITION

Recent investigators (*3*) have observed no inhibition of the decomposition reaction on Pt by N_2 although from our results it appears that they had insufficient accuracy or used temperatures and pressures where N_2 inhibition was small. Figure 10 shows the reaction rate at NH_3 pressures of 0.8 and 1.9 Torr for nitrogen pressures indicated.

Assuming N_2 inhibition of the form of Eq. (8), the pressure dependence of the inhibition term is shown in Fig. 11. The scatter is larger than for H_2 because inhibition is smaller, but at the four temperatures shown the data are consistent with a first-order dependence. The Arrhenius plot of K_N versus $1/T$ in Fig. 12 gives a straight line, and from these figures we obtain

$$K_N P_{N_2}^{m_N} = 1.25 \times 10^{-3} \times \exp(12{,}600/RT) P_{N_2}. \quad (11)$$

The curves shown in Fig. 10 are those *calculated* from Eq. (8) with parameters from Eqs. (5), (7), and (11).

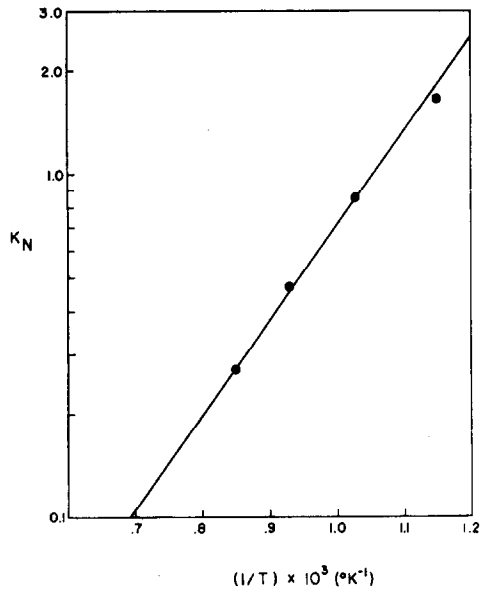

FIG. 12. Plot of log K_N versus $1/T$. Slope and intercept give the parameters in the nitrogen adsorption constant as shown in Eq. (11).

DISCUSSION

It is of course difficult to demonstrate that any particular rate equation gives the "best" fit to experimental data. However, our rate expression

$$r_R\left(\frac{\text{molecules}}{\text{cm}^2\,\text{sec}}\right) = [9.87 \times 10^{18} \exp(-4300/RT)P_{NH_3}]/[1 + 4.35 \times 10^{-5} \exp(16{,}700)/RT)P_{NH_3} + 9.85 \times 10^{-6} \exp(27{,}700/RT)P_{H_2}^{\frac{3}{2}} + 1.25 \times 10^{-3} \exp(12{,}600/RT)P_{N_2}] \quad (12)$$

fits all of the data points in pure NH_3 (Fig. 2) and in NH_3/H_2 or NH_3/N_2 mixtures (Figs. 6 and 9) to within a few percent. This expression is valid over a factor of 10^3 in pressure, temperatures between 500 and 1700°K, rates varying by a factor of 10^4, and hydrogen inhibition of the reaction rate by a factor of 10^2. This expression is certainly an adequate representation of the experimental results, although any temperature dependences of pre-exponential factors would be averaged in Arrhenius plots. Also, the nitrogen inhibition is so small that its pressure dependence is certainly not determined uniquely from these experiments. However, it should be noted that over the wide range of the experimental variables, no systematic deviations from the calculated curves at the extremes of these variables are evident.

Kinetics and Mechanisms

Since this rate expression is a very simple one and has the general Langmuir–Hishelwood form, one might expect that it is possible to use it to describe the rate steps in the reaction and the dominant adsorbed complexes. In this section we shall consider several mechanisms which can lead to the observed kinetics. However we shall see that an expression of this form is obtained only with rather restrictive assumptions on coverages which may not be reasonable for the wide range of temperature and composition over which the rate expression is valid.

The simplest rate formulation assumes single rates and coverage-independent parameters. This approximation we shall term LH kinetics, although we shall not necessarily assume adsorption–desorption equilibrium. Next in complexity, one allows heats of adsorption to be functions of coverage, and finally all parameters may be considered to be dependent on densities of all species. The former leads, with certain site distribution functions, to Temkin–Pyzhev kinetics (*9*). The latter has received little attention, although clean surface adsorption studies show that the interaction between coadsorbed species is frequently very complex. Because of the simple form of Eq. (12), we infer that mechanisms involving LH kinetics should be adequate to explain the results. Temkin–Pyzhev kinetics can give an expression of

the above form in limiting cases, but the observed simple orders would be only coincidental.

While all models considered here have been discussed in the literature in various forms, all have used rather restrictive assumptions (a high pressure of H_2, high or low temperatures, coverages of particular species rather very low or very high) so that rate expressions should at best be valid only over a limited region of composition and temperature. An additional limitation arises when one attempts to include the coverage dependence of sticking coefficients. If coverages are not assumed to be small under all conditions, then rate expressions are sensitive to the coverage dependences of the sticking coefficients [$s \sim 1 - \theta$, $(1 - \theta)^2$, precursor, etc.] and to whether adsorption is competitive or not. None of these parameters is known for the adsorbates of interest here, and one can only make assumptions regarding them.

There are many possible surface complexes including partially dissociated NH_3 residues and species with N–N bonds. Ignoring the latter, the steps in the reaction probably are

$$NH_3(g) \rightleftarrows NH_3(s) \rightleftarrows NH_2(s) \rightleftarrows NH(s) \rightleftarrows N(s) \rightleftarrows N_2(g). \quad (13)$$

This sequence involves 12 rate constants, unknown orders of desorption processes, and coverage dependences of sticking coefficients. It is therefore impossible to ascertain which steps are rate limiting and which are in equilibrium from the general sequence which gives these kinetics.

Rates at low H_2 pressures. In pure NH_3 the data of Fig. 2 are fit very well by Eq. (2). This expression is obtained for almost any rate limiting steps in the limit of low hydrogen and nitrogen coverages, and it shows only that the rate step could not be a bimolecular one such as $r \simeq k\theta_{NH_3}^2$. Writing the reaction steps as

$$\begin{aligned} &(1) \quad NH_3(g) \underset{k_d}{\overset{k_a}{\rightleftarrows}} NH_3(s), \\ &(2) \quad NH_3(s) \xrightarrow{k_R} \tfrac{1}{2}N_2(g) + \tfrac{3}{2}H_2(g), \end{aligned} \quad (14)$$

the rate of reaction is

$$r_R = \frac{[k_R k_a/(k_d + k_R)P_{NH_3}]}{[1 + k_a/(k_d + k_R)P_{NH_3}]}, \quad (15)$$

where k_a, k_d, and k_R are rate constants for adsorption, desorption and reaction, respectively. Step (2) in Eq. (14) represents a sequence of steps which, in the absence of surface hydrogen and nitrogen, is irreversible. In both first- and zero-order regimes, the observed rate constants apparently have Arrhenius forms, but it is not possible to distinguish whether k_d or k_R dominates in Eq. (15). If $k_R \ll k_d$, then K_{NH_3} is a true adsorption–desorption equilibrium constant for NH_3, while if $k_d \ll k_R$, the rate constant at high temperature is k_a. It is necessary to consider finite hydrogen coverages to distinguish between possible reversible and rate-limiting steps in Eq. (13).

Reversible steps involving hydrogen or nitrogen. If the only adsorbed species are H, N, and a single residue of NH_3, termed NH_x with x an integer, then the steps in the reaction may be written (*17*)

$$\begin{aligned} &(1) \quad NH_3(g) \rightleftarrows NH_x(s) + (3 - x)H(s) \\ &(2) \quad NH_x(s) \rightarrow N(s) + xH(s) \\ &(3) \quad 2H(s) \rightleftarrows H_2(g) \\ &(4) \quad 2N(s) \rightleftarrows N_2(g). \end{aligned} \quad (16)$$

The rate of reaction is assumed to be limited by the decomposition rate of this species, step (2), to give

$$r_R = k_2\theta_{NH_x}, \quad (17)$$

and the coverage of NH_x, θ_{NH_x}, is obtained

assuming it to be in a steady state,

$$k_{a1}P_{NH_3}(1 - \theta_{NH_x} - \theta_H) = k_{d1}\theta_{NH_x}\theta_H^{3-x} + k_2\theta_{NH_x}, \quad (18)$$

with rate constants for adsorption and desorption for steps j written as k_{aj} and k_{dj}, respectively. The desorption kinetics in reactions (1) and (2) have been written as proportional to $\theta_{NH_x}\theta_H^{3-x}$ and θ_{NH_x} to obtain analytical solutions, but the actual orders of the processes are of course not known. Equation (18) can be regarded as arising from equilibrium in step (1) which would be determined by stoichiometry.

Solution of Eq. (18) for θ_{NH_x} yields a reaction rate

$$r_R = \frac{(k_2k_{a1}/k_{d1})P_{NH_3}(1 - \theta_H)}{1 + (k_{a1}/k_{d1})P_{NH_3} + (k_{d1}/k_{a1})\theta_H^{3-x}}. \quad (19)$$

Assumption of equilibrium in hydrogen adsorption and desorption with $\theta_{NH_x} \ll 1$ yields

$$\theta_H = \frac{[(k_{a3}/k_{d3})P_{H_2}]^{\frac{1}{2}}}{1 + [(k_{a3}/k_{d3})P_{H_2}]^{\frac{1}{2}}}, \quad (20)$$

and, with $\theta_H \ll 1$, Eq. (17) becomes

$$r_R = \frac{k_2K_{NH_3}P_{NH_3}}{1 + K_{NH_3}P_{NH_3} + \frac{k_{d1}}{k_2}(K_HP_{H_2})^{(3-x)/2}}, \quad (21)$$

with $K_{NH_3} = k_{a1}/k_{d1}$ and $K_H = k_{a3}/k_{d3}$.

Our data are consistent with this expression with $x = 0$, but this model must be invalid for this case because step (2) in Eq. (16) does not exist unless $x \geq 0$. A further difficulty with this expression is that it requires $\theta_H \ll 1$ and, according to Eq. (20), this is not valid at low temperatures. For $\theta_H \simeq 1$, the hydrogen term in the denominator of Eq. (19) becomes independent of P_{H_2}. Also, the term $1 - \theta_H$ of Eq. (19) is $[1 + (k_{a3}/k_{d3}P_{H_2})^{\frac{1}{2}}]^{-1}$, so that Eq. (21) must be multiplied by this term if θ_H is not small.

Many investigators, following Winter (*17*), have assumed that in the decomposition reaction on Fe the rate is limited by the desorption of nitrogen atoms. For the reaction steps

$$\begin{aligned} &(1)\ NH_3(g) \rightleftarrows N(s) + 3H(s) \\ &(2)\quad 2H(s) \rightleftarrows H_2(g) \\ &(3)\quad 2N(s) \rightarrow N_2(g) \end{aligned} \quad (22)$$

a steady-state balance on nitrogen containing species and $\theta_H \ll 1$ yields

$$r_R = \frac{k_{a1}P_{NH_3}}{1 + \frac{k_{a1}}{k_{d3}}P_{NH_3} + \frac{k_{d1}}{k_{d3}}\frac{k_{a4}}{k_{d4}}P_{H_2}^{\frac{1}{2}}}. \quad (23)$$

This expression gives the observed NH_3 and H_2 pressure dependences only if in Eq. (22-3) the rate of nitrogen desorption is written as $k_{d3}\theta_N$ rather than as second order which the stoichiometry would suggest. Also, nitrogen is known to adsorb only weakly if at all on Pt and other fcc metals (*18*), and this implies that nitrogen desorption may be fast.

We thus have two mechanisms which can give the observed rate expression, although only the second, Eq. (22), is consistent with the assumptions used in its derivation. It is easy to modify the assumptions used above, for example, by changing the orders with respect to coverages in adsorption, desorption and reaction steps, but these usually give quadratic or cubic equations which must be solved to obtain coverages explicitly.

We have also considered a number of additional approximations on equilibrium and rate-limiting steps and various site-blocking models, but we have been unable to find rate expressions which are consistent with the experimental rate expression. We have also tested several other rate expressions but found systematic deviations from the data in various ranges of T, P, or composition.

We conclude from these models that reaction kinetics using single states and constant parameters are capable of describing the kinetics quantitatively in that only one term in the numerator is necessary, orders are integral or rational fractions, and coefficients of pressures have Arrhenius temperature dependences. In fact, these models are only slight variations of basically the same process, Eq. (13). However, although these results appear to eliminate several reaction mechanisms, we hestiate to interpret agreement with a particular rate expression as proof that any particular mechanism is operative.

One important conclusion from the quantitative agreement with this simple expression is that kinetics of reactions can be described accurately without resorting to interpretations using variable heats of adsorption or site distributions. If such effects exist they do not affect the rate expression by more than 20%, although these may be included as averages in fitting to the experimental data. In this regard it should be noted that reaction rates are sensitive to particular parameters only in limited ranges of variables. As examples, the activation energy of K_{H_2} is measured *only* at low temperatures and high H_2 pressures, k_R is measured *only* at low temperatures and low H_2 pressures, and $k_R K_{HN_3}$ is measured *only* at high temperatures and low H_2 pressures. From the latter two conditions, k_R could probably be different at low and high temperatures and straight lines in Arrhenius plots could still be obtained.

Reaction Probability and Adsorption Parameters

The probability of reaction of an incident NH_3 molecule,

$$p_R = r_R/\text{flux} = r_R(2\pi MRT_g)^{\frac{1}{2}}/P_{NH_3}, \quad (24)$$

is shown in Fig. 13 for the NH_3 and H_2 pressures indicated. Curves shown are obtained from the rate equation, although individual data points do not deviate significantly from the curves. At high temperatures ($T > 1000°K$ in pure NH_3 and 1400°K with H_2), the reaction probability is independent of pressure or composition and varies between 2×10^{-3} at 1100°K and 3.5×10^{-3} at 1700°K. Hydrogen inhibition at low temperatures, with equal pressures of NH_3 and H_2, is seen to reduce the reaction probability by a factor of ~ 100 or to increase the temperature necessary for a given probability by $\sim 200°K$.

If the denominator terms in the rate of Eq. 8 are interpreted as adsorption–desorption equilibrium constants, then for localized adsorption of a nondissociated species

$$K_A = K_{0A}e^{E_{dA}/RT} = \frac{s_0}{\nu_0^{(1)}(2\pi MRT_g)^{\frac{1}{2}}} e^{E_{dA}/RT}, \quad (25)$$

and for a dissociated species

$$K_A = K_{0A}e^{E_{dA}/RT} = \frac{s_0}{\nu_{d0}^{(2)} n_0 (2\pi MRT_g)^{\frac{1}{2}}} e^{E_{dA}/RT}. \quad (26)$$

In these expressions s_0 is the zero coverage sticking coefficient, ν_0 is the desorption pre-exponential factor, and n_0 is the saturation density.

The pre-exponential factor for nondissociative adsorption is

$$K_{0A}^{(1)} \simeq 10^6 (s_0/\nu_{d0}^{(1)})\text{Torr}^{-1}, \quad (27)$$

and, if $\nu_{d0}^{(1)} \simeq \nu_0$, a vibrational frequency, one obtains $K_{0A} \simeq 10^{-6}$ Torr^{-1} for $s_0 = 1$ and $\nu_0 = 10^{12}$ sec^{-1}. For NH_3, Eq. (12) gives $K_{0NH_3} = 4 \times 10^{-5}$ Torr^{-1} and $E_{dNH_3} = 16{,}800$ kcal/mol, in reasonable agreement with the calculated value of the pre-exponential factor and estimates of the heat of adsorption of NH_3 (*18*). For N_2 the fit was attained for nondissociative adsorption. The value of K_{0N} is above the calculated value by a factor of 10^3, and the heat of adsorption, 12,600 cal/mol, is reasonable for weak chemisorption.

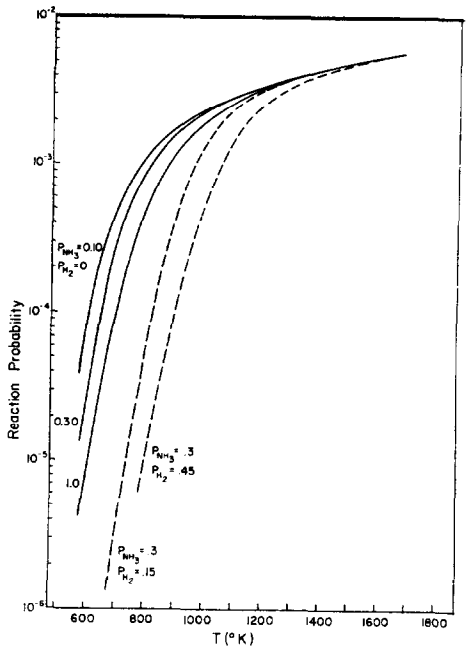

FIG. 13. Plot of reaction probability versus T for NH_3 and H_2 pressures indicated. Above 1000°K the probability is ~ 3–4×10^{-2}, but at lower temperatures it is strongly dependent on P_{NH_3} and P_{H_2}.

For a dissociated species the adsorption–desorption equilibrium constant, defined as in Eq. (20), is

$$K_{0A}^{(2)} = \frac{s_0}{\nu_0^{(2)} n_0 (2\pi MRT)^{\frac{1}{2}}}$$

$$\simeq 10^6 \frac{s_0}{\nu_0^{(2)} n_0} \text{ (Torr}^{-1}\text{)}. \quad (28)$$

The desorption pre-exponential factor $\nu_0^{(2)}$ should be $\simeq 10^{-2}$ cm^2/molecule^{-1} sec^{-1} for localized adsorption (*19*), and with $s_0 = 1$ and $n_0 = 10^{15}$ molecules cm^{-2} one obtains $K_{0A} \simeq 10^{-7}$ Torr^{-1}. Associating the hydrogen term in Eq. (12) with $(K_H^{\frac{1}{2}} P_H^{\frac{1}{2}})^3$ we predict $K_{0A} = 3.1 \times 10^{-8}$ and obtain a heat of adsorption of $\frac{2}{3} \times 27{,}700 = 18{,}500$ cal mol^{-1}. The situation for hydrogen is, however, far from obvious because in many of the possible mechanisms of hydrogen inhibition the denominator term containing P_{H_2} is not associated simply with a hydrogen adsorption–desorption equilibrium constant.

We conclude that our experimental parameters are in satisfactory agreement with calculated pre-exponential factors and experimental heats of adsorption. The major uncertainties in these comparisons are probably in the theoretical quantities. In kinetic derivations one must assume values of ν_0 and s_0, and in statistical mechanical derivations (*20*) even less is known about partition functions for vibration, translation, and rotation.

Comparison with Previous Results

As indicated in Table 1, our results are in remarkably good agreement with most previous experimental studies of NH_3 decomposition on polycrystalline Pt. However, all of these measured rates at only restricted pressures (Apel'baum and Temkin (*3*) used only 0.011 Torr) and all described problems with reproducibility which they attributed to contamination. Further, most experiments were in batch reactors with increasing hydrogen partial pressures as the reaction proceeded; consequently at low temperatures essentially all data were obtained in the presence of large hydrogen inhibition.

Robertson and Willhoft (*7*) made measurements in "high vacuum" ($P_{NH_3} \sim 10^{-4}$ Torr) and in "ultrahigh vacuum" ($P_{NH_3} \sim 10^{-7}$ Torr), and their high temperature results agree very well with ours, although they reported only reaction probabilities rather than the dependence on pressures and gave major emphasis to activation and deactivation processes. Agreement implies that at high temperature a single rate expression describes the reaction between 10^{-7} and 20 Torr, a range of over 10^8 in reactant pressure.

Apel'baum and Temkin (*3*) display their data mainly in tables, and our rate expression fits their conversion versus time

TABLE 1

Comparison of Reaction Rate Parameters

Conditions	Investigators	E (kcal/mol)	m_{NH_3}	m_H	Reaction probability at 1200°K	Pressure (Torr)
High T ($m_H \simeq 0$)	Present work	4.3	0.99 ± 0.05	—	3.3×10^{-3}	0.01–20
	Apel'baum and Temkin (*3*)	5.1	1	—	3.5×10^{-3}	0.0115
	Robertson and Willhoft (*7*)	4.1	—	—	8.9×10^{-3}	$\sim 10^{-4}$
	Robertson and Willhoft (*7*)	4.1	—	—	3.5×10^{-3}	$\sim 10^{-7}$
Low T, low p_{H_2}	Present work	21.1	0.0	—	—	0.015–20
	Robertson and Willhoft (*7*)	17–23	—	—	—	10^{-4}
	Robertson and Willhoft (*7*)	50–60	—	—	—	10^{-7}
Low T, high p_{H_2}	Present work	32.1	1.0	-1.5 ± 0.3	—	0.05–2.6
	Apel'baum and Temkin (*3*)	49.3	1.46	−2.19	—	0.0115
	Dixon (*8*)	40	—	—	—	769
	Melton and Emmet (*10*)	52	1	−1	—	0.005–0.015

results at low temperatures moderately well (within a factor of 10 or with temperature differences of $<100°$ for identical rates). Although our data do not agree with their low temperature rate expression, the two sets of data appear to be generally consistent.

SUMMARY

We have measured NH_3 decomposition rates with a precision comparable to that usually attained in homogeneous kinetics and over a range of variables limited only by the vaporization of Pt and mass transfer limitations. These rate measurements may therefore be regarded as essentially "complete" in the sense that significant improvements in measurement techniques (from the present $\pm 10\%$ to perhaps $\pm 1\%$) require a sophistication which would be very difficult to achieve and the only kinetic variables not covered are extension to lower pressures and temperatures where no significant changes are anticipated.

All of these results can be correlated with a single rate expression of the LH form, and this demonstrates that it is not necessary to invoke surface heterogeneities on coverage-dependent parameters to fit the rate quantitatively. However, while the data clearly show that certain mechanisms are not operative (Temkin–Pyzhev kinetics or a second desorption process, for example), it is still not possible to describe unequivocally the steps in the reaction or to show that the assumed rate expression gives a unique fit to the data. Additional theoretical and experimental considerations of the adsorption and reaction processes are needed to compare experimental rate parameters with the microscopic variables.

Crystallographic and binding-state averaging may obscure the details of the reaction steps on a polycrystalline surface, although not in an obvious fashion. Experiments are in progress to examine rates on single crystal planes and in ultrahigh vacuum where surface coverages may be

measured directly. However we find that such effects are evident mainly as differences in reaction rates between crystal planes, at least for this rather simple reaction.

More complete description of reaction mechanisms will probably not be attainable through more extensive kinetic measurements but rather through additional, perhaps spectroscopic, methods of characterizing surface species present under reaction conditions.

REFERENCES

1. Frankenburg, W. G., *in* "Catalysis" (P. H. Emmett, Ed.), Vol. 3, p. 171. Reinhold, New York, 1955.
2. Bond, G. C., "Catalysis by Metals." Academic Press, New York, 1962.
3. Apel'baum, L. O., and Temkin, M. I., *Russ. J. Phys. Chem.* **33**, 585 (1959).
4. Logan, S. R., and Kemball, C., *Trans. Faraday Soc.* **56**, 144 (1960).
5. Schwab, G. M., and Schmidt, H., *Z. Phys. Chem.* (*Leipzig*) **3B**, 337 (1929).
6. Hinshelwood, C. N., and Burk, R. E., *J. Chem. Soc.* **127**, 1105 (1925).
7. Robertson, A. J. B., and Willhoft, E. M. A., *Trans. Faraday Soc.* **63**, 476 (1967).
8. Dixon, J. K., *J. Amer. Chem. Soc.* **53**, 2071 (1931).
9. Temkin, M., and Pyzhev, V., *Acta Phys.* **12**, 327 (1940).
10. Melton, C. E., and Emmett, P. H., *J. Phys. Chem.* **68**, 3318 (1964).
11. Fogel, J. A. M., Nadikto, B. T., Ribalko, V. F., Slabospitskii, R. P., Korobchanskaja, I. E., and Shvachko, V. I., *J. Catal.* **4**, 153 (1965).
12. Hori, G. K., and Schmidt, L. D., *J. Catal.* **38**, 335 (1975).
13. Pignet, T., and Schmidt, L. D., *Chem. Eng. Sci.* **29**, 1123 (1974).
14. Pignet, T., and Schmidt, L. D., *J. Catal.* **40**, 212 (1975).
15. McCabe, R., Pignet, T., and Schmidt, L. D., *J. Catal.* **32**, 114 (1974).
16. Pignet, T., Schmidt, L. D., and Jarvis, N. L., *J. Catal.* **31**, 145 (1973).
17. Winter, E., *Z. Phys. Chem.* (*Leipzig*) **13B**, 401 (1931).
18. Hayward, D. O., and Trapnell, B. M. W., "Chemisorption." Butterworths, Washington, D.C., 1964.
19. Schmidt, L. D., *in* "Catalysis Reviews" (H. Heinemann and J. J. Carberry, Eds.), Vol. 9, p. 115. Marcel Dekker, New York, 1974.
20. Hill, T. L., "An Introduction to Statistical Thermodynamics." Addison-Wesley, Reading, Mass., 1960.